

Gravitomagnetic Effect in Magnetars

Debarati Chatterjee*

LPC/ENSICAEN, 6 Boulevard Maréchal Juin, 14050 Caen, France

Chandrachur Chakraborty†

Tata Institute of Fundamental Research, Mumbai 400005, India

Debades Bandyopadhyay‡

Astroparticle Physics and Cosmology Division,

Saha Institute of Nuclear Physics, HBNI, Kolkata 700064, India

Abstract

Rotating bodies in General Relativity produce frame dragging (or Lense-Thirring effect), also known as the *Gravitomagnetic effect* in analogy with Classical Electromagnetism. In this work, we study the effect of strong magnetic fields in neutron stars on the Gravitomagnetic effect, which is produced as a result of its rotation. We show that the magnetic field has a non-negligible impact on frame dragging. The maximum effect of the magnetic field appears along the polar direction, where the Lense-Thirring frequency decreases with increase in magnetic field, and along the equatorial direction, where its magnitude increases. For intermediate angles, the effect of the magnetic field decreases, and goes through a minimum for a particular angular value at which magnetic field has no effect on Gravitomagnetism. Beyond that particular angle Gravitomagnetic effect increases with increasing magnetic field. We try to identify this “Null Region” for the case of magnetars, both inside and outside, as a function of the magnetic field. We demonstrate a thought experiment to find the magnetic field and the null region of a particular pulsar using the frame dragging effect.

Key words : rotating neutron stars, frame dragging, magnetic field

1 Introduction

Neutron stars are ideal testing grounds for studying strong gravitational effects as predicted by General Relativity. The dragging of inertial frames is one such important relativistic effect in compact stars. As the surrounding spacetime of a rotating compact object is dragged due to its rotation, the nearby spacetime is basically distorted due to this effect. General relativity predicts that the curvature of spacetime is produced not only by the distribution of mass-energy but also by its motion. Similarly, in electromagnetism, the fields are produced not only by charge distributions but also by currents, i.e., as the moving charge produces the magnetic field. Considering this analogy, this effect is also called the *Gravitomagnetic effect*. Spacetime is distorted by its mass as well as by its rotation. If a small part of the matter starts to rotate, the inertial frame must be dragged along slightly. The small rotation of the earth also drags the local inertial frame along it. Lense and Thirring [1] first discovered that the rotation of a massive body could distort the spacetime, making the spin of nearby test gyroscope precess [2]. This does not happen in Newtonian gravity for which the gravitational field of a body depends only on its mass, not on its rotation. This dragging frequency depends on the angular momentum of the rotating object as well as its compactness, hence its value is large for rapidly rotating neutron stars. Thus the strong gravitational field in the vicinity of neutron stars may

*dchatterjee@lpccaen.in2p3.fr

†chandrachur.chakraborty@tifr.res.in

‡debades.bandyopadhyay@saha.ac.in

provide an opportunity to observe and identify frame dragging effects. As this effect decreases as the inverse cube of the distance from the source, the frame dragging rate is expected to be largest at the vicinity of the centre of a rotating neutron star and falls off with inverse cube law of distance toward the surface and the distance away from it in weak gravity regime.

Lense-Thirring (LT) precession is generally studied in the context of the accretion disc theory where the orbital plane precession frequency is calculated for a *test particle* orbiting in the equatorial plane relative to the asymptotic observer. In this article, we derive the LT precession frequency of a test gyroscope (*spinning test particle*) relative to the “fixed stars” (Copernican system) which was first proposed in [2]. He derived the LT precession frequency of a test gyroscope relative to the “fixed stars” for a rotating spacetime in the weak-field regime. A test gyro follows the gyroscope equation and not necessarily follows a geodesic path in the presence of gravitational fields. Therefore, it is more general than the LT frequency of a test particle moving in a geodesic. It may be useful to mention here that Chakraborty and Majumdar derived [3] the exact LT precession rate of a test gyro in Kerr spacetime without invoking the weak field approximation and showed that the exact formulation reduced to the well-known LT frequency rate in weak gravity regime, derived in [2]. In this article, we will deal with the exact LT precession rate of a *spinning test particle* due to the rotation of a pulsar. We should mention that based on the proposal by Schiff, the Gravity Probe B experiment had been designed to measure the frame-dragging effect of a test gyroscope (relative to the Copernican system or “fixed star” HR8703, also known as IM Pegasi) due to the rotation of the Earth [4] to very high accuracy. The former LAGEOS satellite provided a low precision measurement of the LT precession of the orbit. However the prospect of measurement of LT frequency of a test gyroscope due to the rapidly rotating neutron stars is attractive, as the frame-dragging precession in neutron stars is larger than the precession due to oblateness. Further, as the frame dragging effect is also found to occur inside rotating neutron stars and the magnitude of this effect depends on the density profile, it is an interesting prospect to try to constrain the equation of state exploiting this effect [5, 6]. The matter orbits in accretion disks can provide ways to probe the spacetime properties in the vicinity of neutron stars, including frame dragging effects. Quasi-periodic oscillations (QPOs) observed in X-ray Bursts and diagnostics of X-ray spectra have been suggested as promising tools to investigate the motion of matter around neutron stars [7]. Recently, it has been predicted [8] that frame-dragging can be generated by the electromagnetic fields. In this article they have basically calculated the *orbital plane precession frequency* considering an *orbiting test particle*.

Using the slow-rotation approximation proposed in [9], the frame dragging effect inside a slowly rotating neutron star can be estimated. In this approximation, to second order in rotation frequencies, the structure of a star changes only by quadrupole terms and the equilibrium equations describing the structure reduce to a set of ordinary differential equations. The frame-dragging frequency in this scheme is only a function of the radial distance from the centre of the star. The precession frequency at the centre is then given by the frequency of rotation of the neutron star, and drops off monotonically towards the surface. In a recent investigation, the exact LT frequency of a test gyro was derived in [10]. The frame dragging rate was found to be not only a function of the rotation frequency of the star but also of the other metric components. Unlike in the slow rotation limit, it was found that the precession rate depends both on the radial distance (r) and the colatitude (θ) of the gyroscope. Thus, in rapidly rotating neutron stars, the precession rates are not found to be the same in the equatorial and polar directions.

It is well known that neutron stars are endowed with strong magnetic fields. The surface magnetic field value for normal pulsars, estimated from their spin down rates, points to values around $10^{12} - 10^{13}$ G. There have been reports of discovery of high magnetic field neutron stars, both in isolated systems (XDINSs, RRATs) [11, 12] as well as in binaries (SXTs) [13]. The largest magnetic fields have been observed in Anomalous X-ray Pulsars (AXPs) and Soft Gamma-ray Repeaters (SGRs), commonly called magnetars. Various observations, including direct detection of cyclotron features in the spectra

[14, 15] confirm that these objects possess surface magnetic fields as large as $10^{15} - 10^{16}$ G. However, magnetic fields in the interior of magnetars could be even larger. As it cannot be directly measured, the maximum interior magnetic field is usually estimated using the scalar virial theorem, which points towards a value of 10^{18} G. The presence of a strong magnetic field breaks of spherical symmetry of the star, resulting in a strong deformation of its shape from isotropy. The investigation of the effect of strong magnetic fields on the frame-dragging rate in magnetars is the aim of this paper.

The scheme of the paper is as follows. In Sec.2 of this paper, we define the basic equations to describe the exact frame dragging rate in rotating neutron stars in presence of an electromagnetic field. Sec.3 explains the numerical scheme for solving the equations described in the previous section. The results obtained are discussed in Sec.4 and Sec.5 is devoted to demonstrate a thought experiment to determine the magnetic field and the “Null Region” of a pulsar using LT precession. Finally Sec.6 closes the article with a summary and future outlook.

2 Equations for frame dragging rate in rotating neutron stars

To construct numerical models of rotating neutron stars endowed with a magnetic field within a framework of general relativity, we follow the approach of [16]. With the assumption of a stationary, axisymmetric spacetime, in which the matter part fulfils the circularity condition, the line element can be written as [17]:

$$ds^2 = -N^2 dt^2 + A^2(dr^2 + r^2 d\theta^2) + B^2 r^2 \sin^2(d\phi - N^\phi dt)^2 \quad (1)$$

where N, N^ϕ, A, B are functions of (r, θ) . The energy-momentum tensor in the presence of a magnetic field can be written as:

$$T^{\mu\nu} = (\varepsilon + P)u^\mu u^\nu + Pg^{\mu\nu} - \frac{1}{\mu_0} \left(F^{\mu\alpha} F_\alpha^\nu + \frac{g^{\mu\nu}}{4} F_{\alpha\beta} F^{\alpha\beta} \right). \quad (2)$$

Here the first term represents the matter contribution (perfect fluid), where ε is the energy density, P is the pressure and u^μ is the fluid four velocity. The last term gives the electromagnetic field contribution to the energy-momentum tensor. It was shown in [17] that the contributions of magnetization and the magnetic field dependence of the Equation of State (EoS) on the structure of strongly magnetised neutron stars are negligible, hence we disregard them in the calculations.

In the same way as in [18] we consider here that the electromagnetic field originates from free currents, noted hereafter simply j^σ , which are *a priori* independent from the movements of inert mass (with 4-velocity u^μ). This is a limiting assumption in our model, and one should in principle use a microscopic model to derive a distribution for the free currents, too. However, such a model would require a multi-fluid approach to model the movements of free protons and electrons, and we leave it for a future study.

Subject to the symmetries considered in our model, the definition of the electromagnetic field tensor $F^{\mu\nu}$ determines the magnetic field configuration, either purely poloidal or purely toroidal. We choose a purely poloidal configuration. The electric and magnetic fields measured by the Eulerian observer (whose four-velocity is n^μ) are then defined as $E_\mu = F_{\mu\nu} n^\nu$ and $B_\mu = -\frac{1}{2} \epsilon_{\mu\nu\alpha\beta} n^\nu F^{\alpha\beta}$, with $\epsilon_{\mu\nu\alpha\beta}$ is the Levi-Civita tensor associated with the metric (1). The non-zero components read (see

[17, 18] for detailed calculations):

$$E_r = \frac{1}{N} \left(\frac{\partial A_t}{\partial r} + N^\varphi \frac{\partial A_\varphi}{\partial r} \right) \quad (3)$$

$$E_\theta = \frac{1}{N} \left(\frac{\partial A_t}{\partial \theta} + N^\varphi \frac{\partial A_\varphi}{\partial \theta} \right) \quad (4)$$

$$B_r = \frac{1}{Br^2 \sin \theta} \frac{\partial A_\varphi}{\partial \theta} \quad (5)$$

$$B_\theta = -\frac{1}{B \sin \theta} \frac{\partial A_\varphi}{\partial r}. \quad (6)$$

In presence of an electromagnetic field, the equilibrium configurations for rotating neutron stars are determined by solving the coupled Maxwell-Einstein equations. In the case of rigid rotation, this is equivalent to solving a first integral of the equation of fluid stationary motion [16, 17, 18]:

$$H(r, \theta) + \nu(r, \theta) - \ln \Gamma(r, \theta) + \Phi(r, \theta) = \text{const} \quad (7)$$

taking into account the Lorentz force exerted by the electromagnetic field on the medium, via the electromagnetic term:

$$\Phi(r, \theta) = - \int_0^{A_\phi(r, \theta)} f(x) dx \quad (8)$$

where f is an arbitrary current function relating the components of the electric current to the electromagnetic potential A_ϕ . In the above equation, H is the fluid log-enthalpy, ν is the gravitational potential related to the metric component N ($\nu = \ln N$), while Γ is the Lorentz factor relating the Eulerian observer to the fluid comoving observer.

We recapitulate here the basic equations for the exact frame dragging rate in rotating neutron stars (see [10] for a detailed derivation) using the metric Eq. (1). In the orthonormal coordinate basis, the exact LT precession rate of a test gyro relative to the Copernican system (or “fixed stars”) for the rotating neutron star with electromagnetic field can be written as:

$$\begin{aligned} \vec{\Omega}_{LT} = & \frac{1}{2NA(-N^2 + (N^\phi)^2 r^2 B^2 \sin^2 \theta)} \cdot \\ & \left[\sin \theta [N^2 (BrN_{,r}^\phi + 2N^\phi r B_{,r} + 2N^\phi B) + (N^\phi)^2 r^3 B^3 N_{,r}^\phi \sin^2 \theta - 2N^\phi BrNN_{,r}] \hat{\theta} \right. \\ & \left. - [N^2 (BN_{,\theta}^\phi \sin \theta + 2N^\phi B_{,\theta} \sin \theta + 2N^\phi B \cos \theta) + (N^\phi)^2 r^2 B^3 N_{,\theta}^\phi \sin^3 \theta - 2N^\phi BNN_{,\theta} \sin \theta] \hat{r} \right] \end{aligned} \quad (9)$$

and the modulus of Eq. (9) is

$$\begin{aligned} \Omega_{LT} = & |\vec{\Omega}_{LT}(r, \theta)| \\ = & \frac{1}{2NA(-N^2 + (N^\phi)^2 r^2 B^2 \sin^2 \theta)} \cdot \\ & \left[\sin^2 \theta [N^2 (BrN_{,r}^\phi + 2N^\phi r B_{,r} + 2N^\phi B) + (N^\phi)^2 r^3 B^3 N_{,r}^\phi \sin^2 \theta - 2N^\phi BrNN_{,r}]^2 \right. \\ & \left. + [N^2 (BN_{,\theta}^\phi \sin \theta + 2N^\phi B_{,\theta} \sin \theta + 2N^\phi B \cos \theta) + (N^\phi)^2 r^2 B^3 N_{,\theta}^\phi \sin^3 \theta - 2N^\phi BNN_{,\theta} \sin \theta]^2 \right]^{\frac{1}{2}} \end{aligned} \quad (10)$$

where ‘, r ’ and ‘, θ ’ represent the derivatives with respect to r and θ respectively.

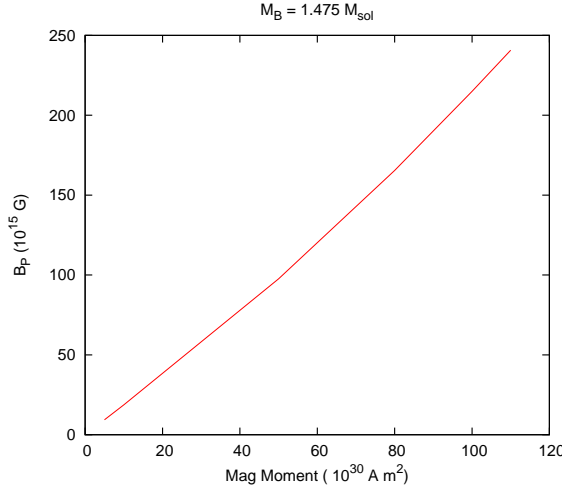


Figure 1: Magnetic moment vs polar magnetic field (B_P) for a non-rotating pulsar having a baryonic mass M_B of $1.475 M_\odot$.

3 Numerical scheme

The Einstein-Maxwell equations described above are solved in the 3+1 formalism, where they reduce to Poisson-like partial differential equations. These equations are then solved numerically using spectral scheme within the numerical library LORENE [19]. The input parameters for the model are an EoS, the current function f , the rotation frequency Ω and the central log-enthalpy H_c . The electromagnetic field originates from the free currents, which are controlled via the current function f . Varying the input current function f allows us to control the intensity of the magnetic field B or the magnetic moment \mathcal{M} . On the other hand, varying the central log-enthalpy permits variation of the mass of the neutron star (gravitational mass M_G or baryon mass M_B).

Using the numerical scheme described above, we compute models of fully relativistic neutron stars for a given magnetic field configuration. We consider a poloidal magnetic field configuration. We choose as an example a particular pulsar PSR J0737-3039 whose mass ($1.337 M_\odot$) and spin ($\Omega = 276.8 \text{ s}^{-1}$) are well known. The exact frame-dragging rate for this pulsar was calculated for the non-magnetic case in [10]. We now study the effect of magnetic field on its frame dragging rate. Just as in the case of a rotating star it is not the rotation frequency but the moment of inertia which is a constant of motion, for strongly magnetised neutron stars the magnetic field is not constant of motion but rather the magnetic moment. To give a clearer correspondence between the polar magnetic field of the pulsar and its magnetic moment, we plot in Fig. 1 the relation between the two for a given baryonic mass of $1.475 M_\odot$, which corresponds to a gravitational mass of $1.337 M_\odot$ for the zero magnetic field case. We can see from the figure that the relation is almost linear, with the largest value $1.1 \times 10^{32} \text{ A.m}^2$ for the magnetic moment corresponding to a magnetic field value of $2.4 \times 10^{17} \text{ G}$.

To show the effect of strong magnetic field on the structure of a neutron star, we demonstrate an equilibrium neutron star configuration corresponding to a magnetic moment of $1.1 \times 10^{32} \text{ A.m}^2$. In Fig. 2, the magnetic field lines (top panel) and enthalpy isocontours (bottom panel) in the meridional plane for PSR J0737-3039, having a gravitational mass of $1.337 M_\odot$ and angular frequency of 276.8 s^{-1} , for a magnetic moment of $1.1 \times 10^{32} \text{ A.m}^2$ have been displayed. It is evident from the figure, that under the influence of the strong magnetic field, the stellar surface has been highly deformed from spherical symmetry.

To estimate the deformation of the structure due to the magnetic field, we compared the values of

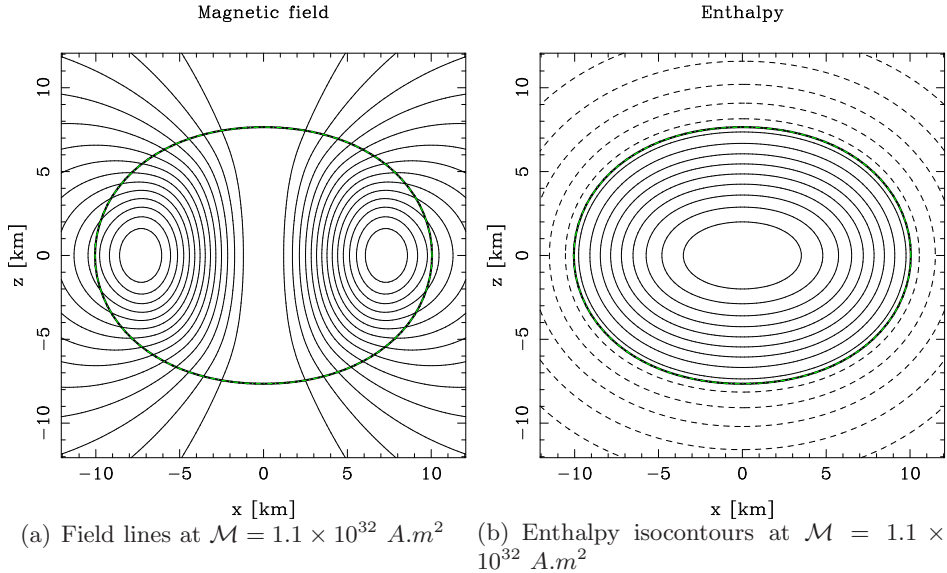


Figure 2: Magnetic field lines (top panel) and enthalpy isocontours (bottom panel) in the meridional plane for PSR J0737-3039, for a magnetic moment of $1.1 \times 10^{32} \text{ A.m}^2$

Table 1: Deformation of strongly magnetized neutron stars for varying magnetic moments \mathcal{M} (in A.m^2). Displayed below are the values of polar to equatorial flattening r_{pole}/r_{eq} , corresponding equatorial circumferential radii R_{circ} (in km) and the quadrupole moments Q (in 10^{38} kg.m^2).

\mathcal{M} (A.m^2)	r_{pole}/r_{eq}	R_{circ} (km)	Q (10^{38} kg.m^2)
5×10^{30}	0.998	11.355	0.00067
10^{31}	0.997	11.361	0.00197
5×10^{31}	0.937	11.540	0.04088
8×10^{31}	0.856	11.815	0.09581
10^{32}	0.793	12.054	0.14013
1.1×10^{32}	0.761	12.189	0.16399

the r_{pole}/r_{eq} and the quadrupole moment of the star due to different constant magnetic moments. The values are displayed in Table 1. It is evident from the table that with increase in magnetic moment, the flattening increases i.e., the ratio of polar radius with respect to the equatorial radius decreases from 1 (for a spherical star). The equatorial circumferential radius as well as the quadrupole moment increase with increase in magnetic field.

4 Results and Discussions

It was shown in [10] that the behaviour of the LT-precession rate for different EoSs is qualitatively similar. Therefore in this study, we employ only the APR [20] EoS. The maximum masses as well as the corresponding radii of static neutron stars as well as those rotating at Kepler frequency were displayed already in [10], hence we do not repeat this study here. Our aim is to perform a study of the effect of magnetic field on the frame dragging rate Ω_{LT} for neutron stars rotating at sub-Kepler frequencies.

We construct equilibrium configurations of neutron stars for constant values of magnetic moment $\mathcal{M} = 5 \times 10^{30}, 10^{31}, 5 \times 10^{31}, 8 \times 10^{31}, 10^{32}, 1.1 \times 10^{32} \text{ A.m}^2$. For a given magnetic moment, we calculate

the value of the frame-dragging precession rate inside ($r \leq r_s$) as well as outside the pulsar ($r > r_s$), where r_s is the distance of the surface of the pulsar from its centre (at the equator $r_s = r_{eq}$; r_{eq} is the equatorial coordinate radius).

We should clarify that the LT frequency can be calculated using Eq. (10) both inside and outside of a pulsar. As all the parameters (A, B, N, N^ϕ) in Eq. (10) are functions of r and θ , the equation is automatically modified by changing the values of r and θ . Inside the pulsar ($r \leq r_s$) all of the above mentioned parameters take the values corresponding to the solution of the Einstein equation with the energy-momentum tensor mentioned in Eq. (2). Outside the pulsar, ($r > r_s$) Eq. (2) reduces to the case with $\varepsilon = P = 0$ in absence of matter and Eq.(1) describes the electrovacuum solution of the Einstein equation. Thus, the frame-dragging formula (Eq. (10)) also gets modified automatically with the corresponding values of A, B, N, N^ϕ and the LT precession rates (for a given angle) are continuous from the centre to the asymptotically large distances as well as on the surface of the pulsar.

One must note that the effect of strong electromagnetic field is two fold:

- (i) Firstly, there is the effect of electromagnetic field directly on the matter and vacuum solutions, given by Eq. (10).
- (ii) Secondly, strong magnetic field causes a deformation of the stellar surface. Thus it affects the radial distance at which the energy density falls to zero, and consequently the LT frequency also shifts at the radial distance at which the matter solution matches the electrovacuum solution.

4.1 Interior region ($r \leq r_s$)

In Panel (a) and Panel (b) of Fig. 3, we display the frame dragging rate as a function of radial distance (r/r_{eq}) for different angular values from 0 (along polar direction) to 90 (equatorial direction) for two different constant magnetic moments. The results are qualitatively the same as obtained in [10]: the frame dragging frequency has a smooth behaviour along the pole from the centre to the surface of the star but the behaviour is quite different along the equator, which is already been explained in [10] and [21]. Along the equatorial direction the frame dragging frequency goes through a “dip” or local minimum at a certain angle, labeled as “critical angle”. In this case, the critical angle occurs around $\sim 60^\circ$. For magnetic moments $\mathcal{M} \leq 10^{31} \text{ A m}^2$, the results are indistinguishable from the non-magnetic case.

Panels (a) to (j) of Fig. 4 reveal that for different values of magnetic moment, depending on the angular direction, the frame dragging rate differs inside the pulsar. Interestingly, the frame dragging rates along the pole ($\theta = 0^\circ$) decrease with increasing the magnetic moments and the reverse effect is seen along the equator ($\theta = 90^\circ$), i.e., an increase in the frame dragging rates with increasing magnetic moments. Therefore, there should exist a ‘crossover angle’ where the effect of the magnetic field on the frame-dragging effect will be ‘null’. Magnetic field of the pulsar does not affect the gravitomagnetic effect in this region, which we can call the “Null Region”. To find the null region we show the evolution of the frame-dragging effect for various magnetic moments (starting from $0 - 1.1 \times 10^{32} \text{ A.m}^2$) from Panel (a) to Panel (j), i.e., from the pole to the equator for every 10^0 interval. The solid red line represents the zero magnetic moment and black dashed line represents the highest magnetic moment considered. In Panel (a) and Panel (j), the deviation between these two lines is maximum which means that frame-dragging rate is affected maximally by the magnetic moment of the pulsar in these two regions. The evolution from Panel (a) to (e) shows that the distance between these two lines decreases if we proceed from the pole (0°) to an angle $\theta \sim 40^\circ$. Deviation is minimum ($\rightarrow 0$) around $\theta \sim 40^\circ$ (Panel (e)). This shows that magnetism has no effect on frame-dragging at this particular angle. If we proceed further from Panel (f) to Panel (j), we see that the deviation between those two lines (solid red and dashed black) again increases but in this case it is in the reverse direction. Thus the maximum effect of magnetic field is along the polar direction (reducing the frame-dragging frequency) and in the

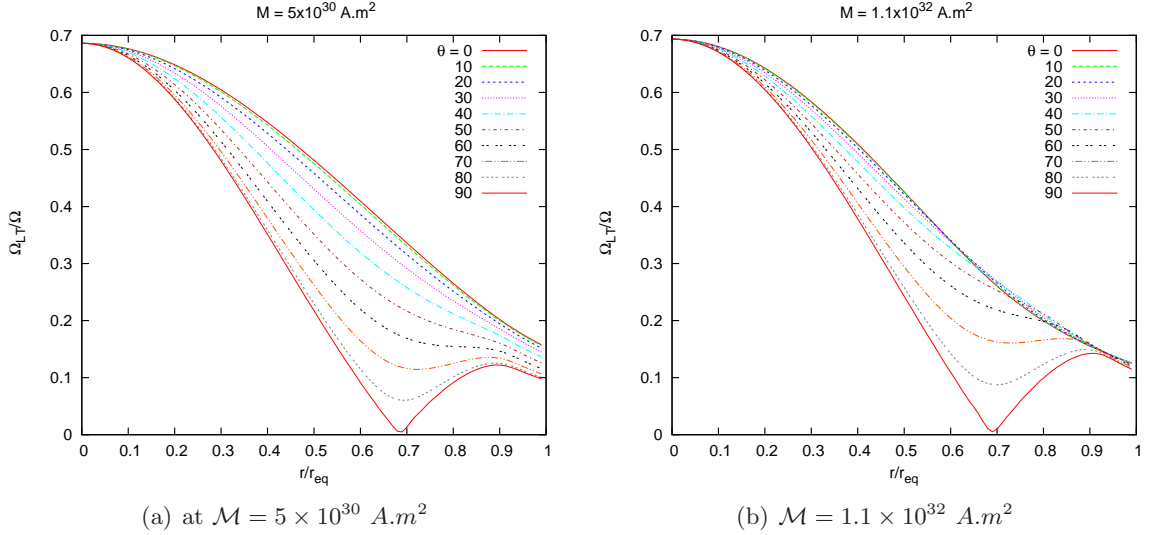


Figure 3: Normalized frame-dragging rate Ω_{LT}/Ω inside the pulsar as a function of radial distance r in units of r_{eq} along the pole ($\theta = 0^\circ$) to equator ($\theta = 90^\circ$) for two values of magnetic moment 5×10^{30} and 1.1×10^{32} $A.m^2$.

equatorial direction (increasing the frame-dragging frequency), while for intermediate angles its effect goes through a minimum, having practically no influence on the frame-dragging frequency around 40° .

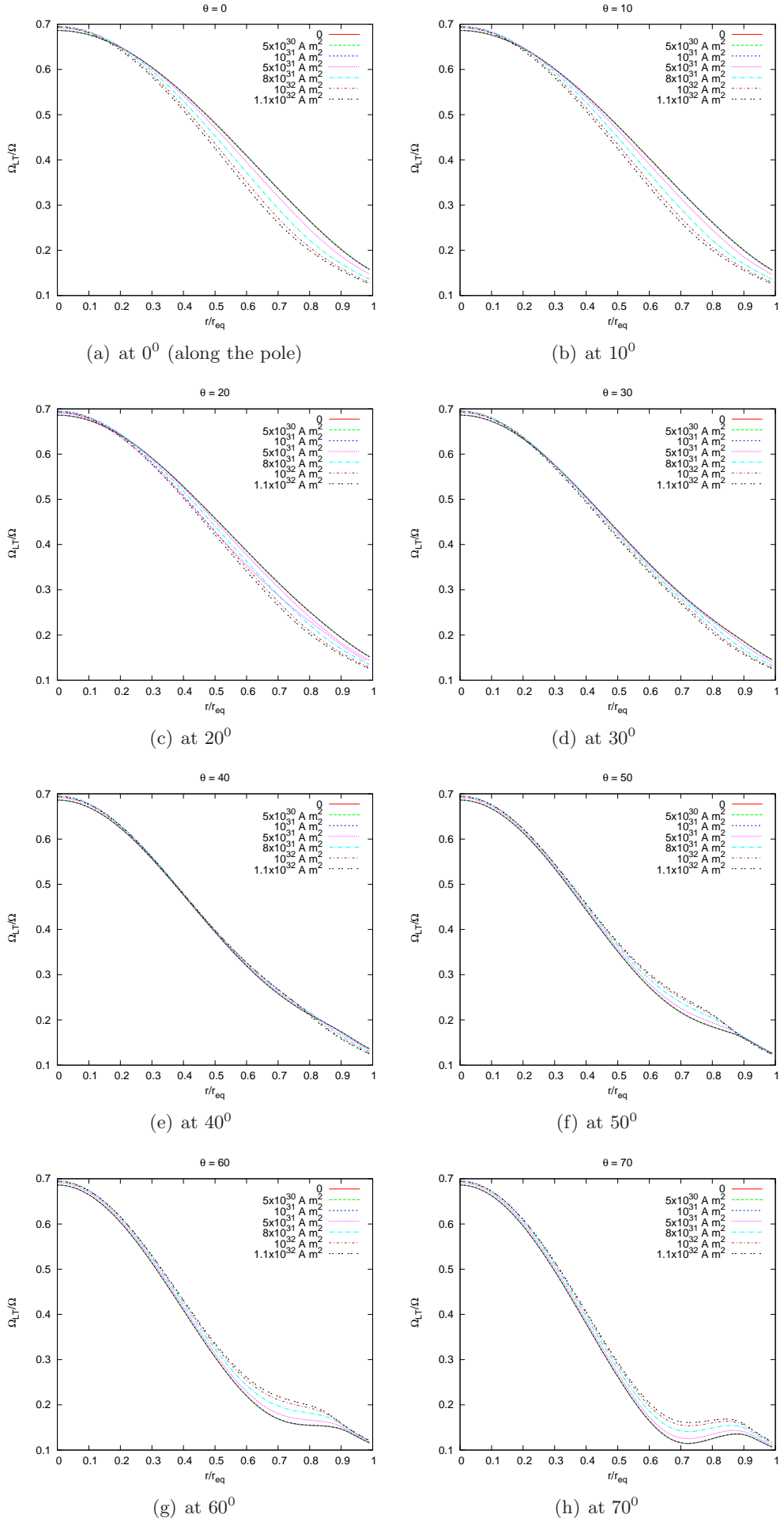
4.2 Exterior region ($r \geq r_s$)

The frame dragging rates are plotted for radial distances extending outside the pulsar ($r \geq r_s$) along polar (panel a), $\theta = 50^\circ$ (panel b) and equatorial directions (panel c) in Fig. (5), respectively. This shows that the null region also exists outside the pulsar, at angle of about 50° . This is expected as the effect of the magnetic field exists not only inside but also outside (in principle $r \rightarrow \infty$) the pulsar and the frame-dragging should therefore also extend upto $r \rightarrow \infty$. The change in the null angle inside and outside can be understood from the fact that, as the energy density vanishes at the surface of the pulsar, the frame-dragging frequency is no longer determined by the matter solution where $T^{\mu\nu}$ is given by Eq. (2) but by the electrovacuum solution with $\varepsilon = P = 0$ in $T^{\mu\nu}$. The curves for frame-dragging frequencies converge asymptotically at large distances ($r \gg r_s$). However, there is an interplay between the influence of the magnetic field on both the matter and vacuum solutions, as well as on the radial distance at which there is a change from the matter to vacuum solutions.

Comparing the energy density profiles along different angles for different magnetic moments, we find that for small values of magnetic moments (e.g. 10^{31} $A.m^2$) the energy density profiles remain the same along all angular directions (see Fig. 6). This is expected as for small magnetic fields the stellar surface remains spherically symmetric. However for large magnetic moments (e.g. 10^{32} $A.m^2$), the energy density profiles vary along different angles (see Fig. 7). This can be understood from the fact that the stellar surface is distorted from spherical symmetry due to the strong magnetic fields. For a poloidal configuration, there is a polar flattening and equatorial bulging, which means the energy density goes to zero at smaller radial distances along the polar direction and at larger radial distances along the equatorial direction, defining the distorted stellar surface. It is found that the energy density profile (and hence the stellar surface) is least affected along 50° (comparing Figs. 6 and 7).

4.3 Role of the rotation frequency of the pulsar

To determine the influence of the value of pulsar rotation on the position of the null region, we repeat the numerical calculations for $\Omega = 0, 100, 1000$ s^{-1} . As the rotation frequency increases to large val-



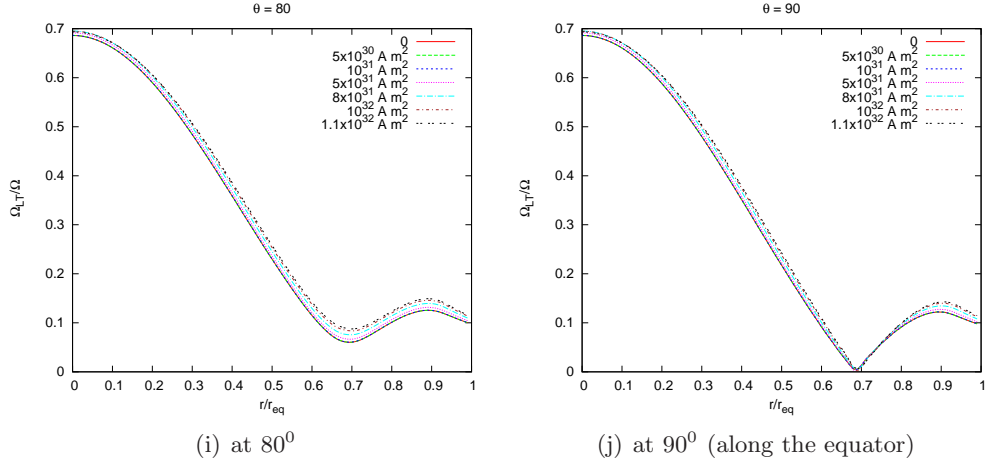


Figure 4: Plot of normalized frame-dragging rate Ω_{LT}/Ω inside the pulsar as a function of radial distance r in units of r_{eq} , from the pole ($\theta = 0^0$) to equator ($\theta = 90^0$) in steps of 10^0 , for different values of magnetic moment.

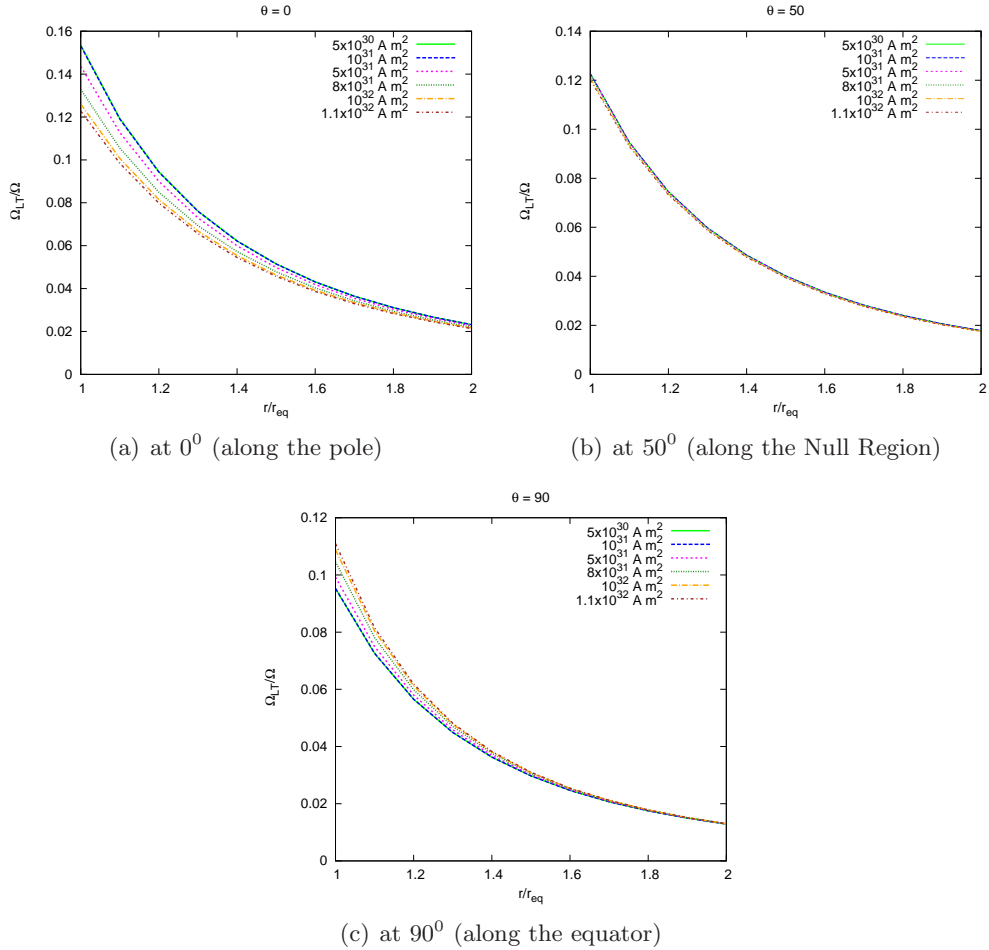


Figure 5: Normalized frame dragging rate Ω_{LT}/Ω vs radial distance r/r_{eq} outside the neutron star along (a) polar direction, (b) Null Region (50^0) and (c) equatorial direction for different values of magnetic moment.

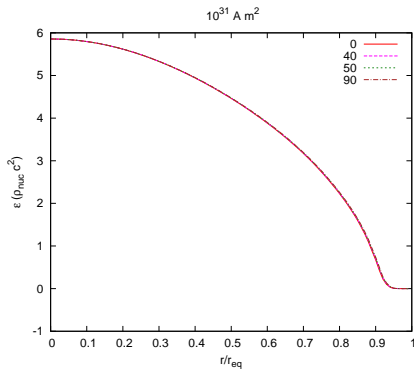


Figure 6: Energy density profile (in units of nuclear density ρ_{nuc}) along polar direction (red solid line), 40^0 (magenta dashed line), at 50^0 (green dotted line) and equatorial direction (brown dot-dashed line) for a magnetic moment of 10^{31} A.m 2 .

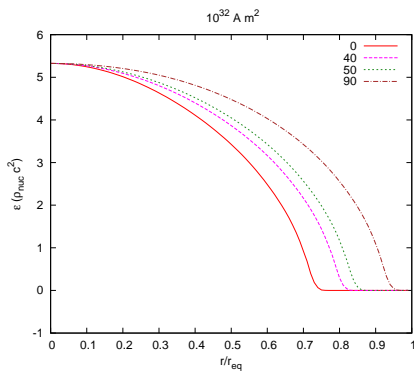


Figure 7: Energy density profile (in units of nuclear density ρ_{nuc}) along polar direction (red solid line), 40^0 (magenta dashed line), at 50^0 (green dotted line) and equatorial direction (brown dot-dashed line) for a magnetic moment of 10^{32} A.m 2 .

ues. the surface of the star is also deformed to a non-spherical shape. However, we found that when the rotation frequency is zero, the LT frequency vanishes, no matter what the value of the magnetic field. This implies that there is no contribution of free precession due to the oblateness caused by the magnetic field, and that the LT effect arises purely due to the rotation of the spacetime. The LT frequency is non-zero only in presence of rotation, and its magnitude is affected by the presence of the magnetic field. However, we have also observed that the value of the rotation frequency of the pulsar has no influence on the value of the angle at which the magnetic field ceases to affect the frame dragging rate. For the interior region, the null region is found at $\sim 40^0$ while for the exterior region it is found at $\sim 50^0$, as obtained for $\Omega = 276.8 \text{ s}^{-1}$ for the PSR J0737-3039.

Here, we should emphasize that any kind of magnetic field is not directly responsible for the frame-dragging effect. This effect solely depends on the rotation of the spacetime (there is also an exception where LT effect is not related to the rotating spacetime but some “rotational sense” was involved ([3]) there). Thus, if a magnetic field exists in a non-rotating spacetime, the spacetime will not be able to show the frame-dragging effect. If the spacetime starts to rotate, gravitomagnetism is induced in this spacetime and the magnetic field comes into play to show its effect on frame-dragging. In an analogy with electromagnetism, we can say that as a non-magnetic material is not affected by the magnetic field of any magnet, the non-rotating spacetime is also not affected by the magnetic field of that spacetime in the case of frame-dragging effect. It is evident from Eq.(1) that N^ϕ vanishes for a non-rotating spacetime ($\Omega = 0$) and therefore the gravitomagnetic effect vanishes ($\Omega_{LT} = 0$) which is also evident from Eq.(9), though the magnetic field is non-zero (see Eq.(2)). The *tussle between magnetic field and gravitomagnetic effect is only possible if they are both present in a particular spacetime*. If any one of them is absent, the tussle will also be absent. That is why it is meaningless to isolate the role of magnetic moment on LT effect from that due to rotation only, but the deviation of the LT effect due to the presence of the magnetic field can easily be deduced from the Panels (a)-(j) of Fig. 4 for various magnetic moment values at various angles.

5 A Thought Experiment to determine the magnetic field and “Null Region” of a Pulsar using LT precession

In the previous section, we have discussed the LT effect of PSR J0737-3039 and without making any realistic experiment we have predicted that the Null region will be at $\sim 40^0$ (inside the pulsar) and $\sim 50^0$ (outside the pulsar) where magnetic field has no effect on Gravitomagnetism, whatever magnetic field value PSR J0737-3039 possesses. The crossover angle of the Null Region between 40^0 to 50^0 occurs on the surface of the pulsar at $\sim 0.8r_{eq}$ which is evident from Panels (e)-(f) of Fig. 4 and Panel (b) of Fig. 5. It is also evident from Fig. 6 that the distance of the surface of the pulsar is $r_s \sim 0.8 r_{eq}$ at 40^0 angle.

In an axisymmetric spacetime, we can imagine that the null angle $2\theta_{in} \sim 2 \times 40^0 = 80^0$ creates a hypothetical 3-D hollow ‘cone’ inside the pulsar and $2\theta_{out} \sim 2 \times 50^0 = 100^0$ outside, which is depicted in Fig. 8. Therefore, if a test gyro moves along the surface of the cone, LT frequency of the gyro will not be affected by the magnetic field of the pulsar whatever magnetic field it holds. If the gyro moves along any direction inside the cone, its LT frequency varies inversely with the magnetic moment and outside the cone the frequency will be directly proportional to the magnetic moment.

Now, using the concept of Gravity Probe B experiment we can demonstrate a thought experiment which can be performed by a test gyro. We can make it move towards the strong gravitational field of a pulsar along the pole or equator or whichever angle we want. For a particular angle outside a unknown pulsar, say, $\theta = \theta_d$, we make the gyro move from *infinity* towards the pulsar and in principle we could measure the exact frame-dragging rate. We could then calculate the difference between this measured frame dragging rate and the theoretically calculated frame dragging rate for zero magnetic field. The difference in the frame dragging along this given angular direction will be determined by

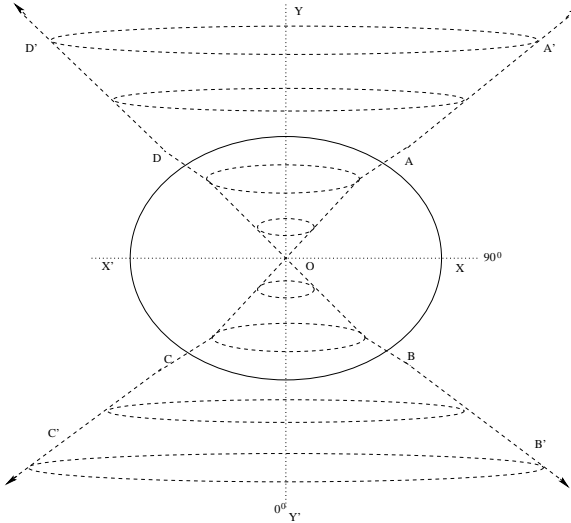


Figure 8: Azimuthal section of a *theoretically predicted* Null Region/Surface of the pulsar PSR J0737-3039 around the symmetry axis $YOY'(0^0)$ or the rotation axis of the pulsar. $X'OX$ is the equatorial plane and solid black line represents the surface of the pulsar. $2\theta_{in} = \angle DOA = \angle BOC \approx 2 \times 40^0 = 80^0$. The boundary of the 3-D hypothetical hollow ‘cone’ has been drawn along $D'DOAA'$ and $B'BOCC'$ around the symmetry axis. In principle, the cone is extended upto $r \rightarrow \infty$, which is shown by four arrows but outside i.e., $0.8r_{eq} < r \leq \infty$ (as $OA = OB = OC = OD \approx 0.8r_{eq}$), the null region appears at $\sim 50^0$ instead of 40^0 which is evident from Panels (e)-(f) of Fig. 4 and Panel (b) of Fig. 5. If the gyro moves along the surface of this 3-D hypothetical ‘cone’, the effect of *magnetic field* of the pulsar will not be exerted on its frame-dragging frequency or gravitomagnetic effect. Inside this cone, Ω_{LT} decreases with increasing magnetic moment and it shows completely reverse effect outside this cone (this figure is not drawn in scale).

the magnetic field of the pulsar. Thus, in principle we can calculate the intensity of the magnetic field of the pulsar in this way. Now, we can move the gyro along different angles θ_d from 0^0 to 90^0 and the angle at which the measured frame dragging frequency is exactly equal to the calculated LT precession frequency for zero magnetic field, is the null angle ($\theta_d = \theta_{out}$) outside the pulsar. As an example, it is 50^0 in Fig. 8. In this way, we can determine the null angle for the effect of magnetic field on LT precession for the particular pulsar. After determining the θ_{out} we can move the gyro further toward the unknown pulsar. Now, very close to the pulsar surface (point A, B, C or D in Fig. 8) we will see that the frame-dragging rate is starting to get affected by the magnetic field suddenly. Now, we have to follow the similar procedure (which we have followed outside the pulsar) at the surface of the neutron star to find the null angle θ_{in} (40^0 in Fig. 8) inside the pulsar.

6 Summary and Outlook

In this work, we extended the recent calculation [10] for exact LT precession rates inside and outside neutron stars to include effects of electromagnetic field. This should be particularly interesting for the case of magnetars, which are strongly magnetised neutron stars, and for the observations of Quasi-Periodic Oscillations (QPOs) in magnetars.

We employed a well established numerical scheme [16, 17, 18] to obtain equilibrium models of fully relativistic strongly magnetised neutron stars. We computed the frame dragging rates inside and outside the stellar surface for such models. We obtained qualitatively similar peculiar features for the frame dragging rates along polar and equatorial directions as previously discussed for non-magnetic calculations [10], with the effect of the electromagnetic field evident on the frame dragging rate inside as well as outside the star. This could be potentially interesting for magnetars for constraining the

magnetic field from a measurement of the LT frequency. As an example for PSR J0737-3039, we found that the maximum effect of magnetic field appears along the polar direction (decreasing the frame-dragging frequency) and in the equatorial direction (increasing the frame-dragging frequency), while for intermediate angles its effect goes through a minimum, having practically no influence on the frame-dragging frequency around 40^0 inside and 50^0 outside the pulsar. We showed that this can be attributed to the twofold effect of a strong magnetic field, on the LT frequency as well as on the breaking of spherical symmetry of the neutron star. We also devised a thought-experiment to determine the magnetic field of the neutron star as well as the null angle using a measurement of its LT frequency.

Measurements of geodetic and frame dragging effects by dedicated missions such as LAGEOS and Gravity Probe B [22] have permitted us to impose constraints and better understand gravito-magnetic aspects of theories of gravity. There is a need to expand the sensitivity of future gravitational tests to neutron stars to understand phenomena such as QPOs and LT precession.

Acknowledgments

One of us (CC) gladly acknowledge Kamakshya P. Modak and Prasanta Char for their valuable suggestions. DC is grateful to Jérôme Novak for his guidance regarding the numerical computation.

References

- [1] Lense, J. and Thirring, H., (1918), *Phys. Z.*, 19, 156.
- [2] Schiff, L. I., (1960), *PRL*, 4, 215; Schiff, L. I., (1960), *American Journal of Physics*, 28, Issue 4, 340.
- [3] Chakraborty, C., Majumdar, P., (2014), *CQG* 31, 075006.
- [4] Everitt, C. W. F. *et. al.*, (2011), *PRL*, 106, 221101.
- [5] Morsink, S. M. and Stella L., (1999), *ApJ* 513, 827.
- [6] Kalogera, V. and Psaltis, D., (2000), *PRD* 61, 024009.
- [7] Stella L. and Possenti A., (2009), *Space Sci Rev*, 2009, 148, 105.
- [8] Gutiérrez-Ruiz, A. F., Pachón L. A., (2015), *PRD*, 91, 124047.
- [9] Hartle, J. B., (1967), *ApJ*, 150, 1005.
- [10] Chakraborty, C., Modak, K. P. and Bandyopadhyay, D., (2014), *ApJ*, 790, 2
- [11] Olausen, S. A. *et al.*, (2013), *ApJ*, 764, 1.
- [12] Ng C.-Y. and Kaspi, V. M., (2011), *AIP Conf. Proc.*, 1379, 60.
- [13] Ho, W. C. G. *et al.*, (2014), *MNRAS*, 437, 3664.
- [14] Ibrahim A. I., Markwardt C. B., Swank J. H., Ransom S., Roberts M., Kaspi V., Woods P. M., Safi-Harb S., Balman S., Parke W. C., Kouveliotou C., Hurley K., Cline T.A.I., (2004), *ApJ*, 609, L21.
- [15] Mereghetti S., (2013), *Braz. J. Phys.*, 43, 356.
- [16] Bonazzola S., Gourgoulhon E., Salgado M., Marck J. A., (1993), *A&A*, 278, 421.
- [17] Chatterjee, D., Elghozi, T., Novak, J. and Oertel, M., (2014), *MNRAS*, 447, 3785.

- [18] Bocquet M., Bonazzola S., Gourgoulhon E., Novak J., (1995), A&A, 301, 757.
- [19] Grandclément P., Novak J., (2009), Living Rev. Relat., 12, 1.
- [20] Akmal A., Pandharipande, V. R., and Ravenhall, D. G., (1998), PRC, 58, 1804.
- [21] Chakraborty, C., (2015), EPJC 75, 572.
- [22] Overduin, J. M., (2015), CQG, 32, 224003.